ORIGINAL PAPER

doi: 10.5455/aim.2024.32.107-111
ACTA INFORM MED. 2024, 32(2): 107-111
Received: NOV 26, 2024
Accepted: DEC 28, 2024

Nguyen Thai Binh[1,2], Le Quy Thien[1], Dang Khanh Huyen[3], Ngo Quang Duy[1], Nguyen Thi Hai Anh4, Le Thanh Dung[5,6], Nguyen Duy Hung[1,6]

[1]1Department of Radiology, Hanoi Medical University, Hanoi, Vietnam

[2]Department of Radiology, Hanoi Medical University Hospital, Hanoi, Vietnam

[3]Department of Radiology, Tam Anh Hospital, Hanoi, Vietnam

[4]Department of Radiology, Alexandra Lepève Hospital, Dunkirk, France

[5]Department of Radiology, VNU University of Medicine and Pharmacy, Vietnam National University, Hanoi, Vietnam

[6]Department of Radiology, Viet Duc Hospital, Hanoi, Vietnam

Corresponding author: Nguyen Duy Hung. Department of Radiology, Hanoi Medical University, Hanoi, Vietnam. E-mail: nguyenduyhung_84@yahoo.com, ORCID ID: 0000-0002-6926-6718.

Assessement of Radiological Anatomy of Prostatic Artery on 3D DECT in Symptomatic Benign Prostatic Hypertrophy

ABSTRACT

Background: Benign prostatic hyperplasia (BHP) is a common disease in the urinary system and often appears in old male patients with the incidence increasing proportionally to age. **Objective:** The study aimed to describe the anatomy and imaging findings of the prostatic artery (PAs) on 3D rendering dual-energy multi-sequence computed tomography (DECT) in patients with symptomatic benign prostatic hypertrophy (BPH) treated by prostatic artery embolisation (PAE). **Methods:** The study was conducted on 64 patients with BPH who underwent DECT scans with 3D rendering of the pelvic artery before intervention from August 2022 to November 2023. The PAs were independently evaluated for each side, focusing on the number of branches, origin, tortuosity, atherosclerotic plaque, and anastomoses with adjacent arteries. **Results:** Among 128 pelvic sides where the PAs can be observed, the rate of finding 01 prostate artery on each side was high (96.1%), and the rate of 02 prostate arteries on each side was rare (3.9%). In 133 prostatic arteries, the most common type of prostatic artery according to origin is type I (29.6%), followed by type III (24.6%). The atherosclerotic prostatic artery rate is 24.6%, and the average diameter is 1.5±0.4 mm. The tortuosity prostate artery accounted for 74.6%. The anastomosis to the contralateral prostatic artery rate is 48.4%, followed by the penis and rectum anastomoses. **Conclusion:** PAs have abundant original varies between the left and right sides and between patient to patient. The most common form arises from the internal pudendal artery.

Key words: dual-energy computed tomography; prostatic artery; DSA.

1. BACKGROUND

Upper Benign prostatic hyperplasia (BHP) is a common disease in the urinary system (1, 2). This illness often appears in old male patients with the incidence increasing proportionally to age. BHP is typically characterized by two common groups of lower urinary tract symptoms (LUTS): lower urinary tract obstruction and lower urinary tract irritation (1). The advent of science has led to the appearance of several management options for BPH with LUTS, encompassing PAE which has been developed over the ten years. There is certainly compelling evidence that highlights the advantages of PAE due to its minimal invasiveness, short-time recovery, low risk of complications and especially suitable for people under anticoagulant therapy, or disqualified to undergo general and spinal anesthesia (2, 3). However, PAE is a challenging technique due to the abundance of anatomical variations (number of branches, origins, and diameters) and differences between patient to patient and side by side in a patient (4, 5). Furthermore, the likelihood of atherosclerosis in the old patient group seriously puts pressure on the interventional process.

In our search of medical literature, there is a large number of investigations of cadaveric prostate artery anatomy, computed tomography angiography (CTA), digital subtraction angiography (DSA), and magnetic resonance angiography (MRA). However, the research field of prostate artery anatomy on multi-sequence dual-energy computed tomography images compared with DSA images is still limited.

2. OBJECTIVE

Therefore, we conducted this paper with the goal of evaluating the value of DECT with 3D rendering of the prostate artery in attempting to describe the

the pre-interventional prostate artery anatomy of symptomatic benign prostate hyperplasia.

3. MATERIAL AND METHODS

Patient Selection

The study was conducted on 64 BHP patients with LUTS at the Department of Radiology of Viet Duc Hospital from August 2022 to November 2023. All the victims received DECT scans with the 3D rendering of the prostate artery before the prostate artery intervention.

Pelvic DECT Protocol

The imaging protocols include obtaining scout views, setting the injection procedure for the iliac artery, and field of view from the iliac crest down to the upper 1/3 of the femur. DECT Revolution HD (GE) imaging parameters in the study: scanning mode (fast switching kV 80/140KV), tube current 600 mA, rotation speed 0.5s, pitch 1.375:1, cutting layer thickness layer thickness 5mm, reconstruction slice thickness 0.625 mm, contrast dose 1.5 ml/kg body weight with contrast injection rate 5ml/s, High DLIR reconstruction algorithm, AW 4.7 processing station. The scanning delay for the mobile phase was determined using automatic scanning trigger software (GE Healthcare). Scanning was performed in simultaneous spectral imaging mode with rapid tube voltage switching between 80kVp and 140 kVp on adjacent views within a single rotation. The image data set reconstructed from the single spectrum acquisition for analysis includes a set of polychromatic images corresponding to conventional 120 kVp images and a set of corresponding monochromatic images at low KeV (40–50 KeV), which is considered optimal for evaluating small arteries.

DSA Protocol

The urinary catheter was inserted for all the patients. Vascular access is through the right brachial artery or femoral artery. A 5 Fr catheter (cobra or vertebral) was selectively placed into the internal iliac artery or anterior branch of the internal iliac artery on each side. An internal iliac angiogram with an oblique view angle similar to the expected angle on MSCT with 3D rendering. A 1.8 – 2.0 Fr microcatheter is used to selectively access the PA on each side. Histoacryl mixed with Lipiodol (ratio 1:4–1:8 depending on each case) is used to embolize bilateral prostate arteries. Postoperatively, the patient is delivered to the clinical department and discharged home on the next day uneventfully

Data analysis

DECT and DSA images were evaluated and analyzed by radiologists with over 5 years of experience in prostatic artery embolization. Particularly, the image of the iliac artery on DECT in terms of quantity, origins, shape and anastomoses has been confirmed in the DSA which is considered as the gold standard for evaluating the DECT images. In this research, quantitative variables are described as average and standard deviation, qualitative variables are described as percentages and numbers. The data were analyzed according to medical statistical methods using SPSS 20.0

4. RESULTS

This research was conducted on 64 patients (equivalent to 128 pelvic sides) who underwent DECT with the 3D reconstruction of the PAs preoperatively. Each pelvic side was evaluated separately regarding the number of PAs, diameter, origin, and quality of arteries. In this study, there was a total of 133 PAs (4 patients had 2 PAs on the right side, and 1 patient had 2 PAs on the left side).

A total of 64 patients undergo PAE from August 2022 to November 2023. The average age of the patients was 67.3 ± 7.8 years old, the average prostate volume was 72.3 ± 12.6 ml, the average IPSS score was 22.2 ± 5.5 points, the average Qol score was 3.4 ± 2.6 points, and the average total PSA concentration was 12.4 ± 5.6 ng/ml.

Among the 128 pelvic sides, a single PA on each side was predominant (96.1%), and double PAs on each side were relatively rare (3.9%). There were no cases with 03 PAs on one pelvic side. The most common type according to the origin was Type I, branching from the common trunk with a superior vesical artery (29.6%). Followed by type III, branching from the obturator artery (24.6%), and Type IV, branching from the internal pudendal artery (23.7%). PAs branching from the anterior branch of the internal iliac artery accounted for 15.4%. There was a minority from other locations (6.7%). The rate of atherosclerosis at the root of the PA was 24.6%. The average diameter of the 133 Pas on DECT was 1.5 ± 0.4 mm.

Characteristic	Mean
Age	67.3±7.8
Prostate Volume	72.3±12.6
IPSS	22.2±5.5
Qol Score	3.4±2.6
Total PSA Concentration	12.4±5.6

Table 1. General characteristics of the patients

Classification		Right (N=68)	Left (N=65)	Total (N=133)	Percent (%)
Number of PAs per Pelvic Side	1 artery	60	63	123	96.1
	2 arteries	4	1	5	3.9
PA Origin According to FC. Carnevale	Type 1	19	20	39	29.6
	Type 2	13	7	20	15.4
	Type 3	15	18	33	24.6
	Type 4	10	22	32	23.7
	Type 5	3	6	9	6.7
Atherosclerosis of the PA Root		18	15	33	24.6
Average Diameter (mm)		1.5±0.4			

Table 2. Classification of PAs by the number on each side of the pelvis, arterial origin and atherosclerosis.

Classification		Right (N=68)	Left (N=65)	Total (N=133)	Percent (%)
Shape	Tortuosity			99	74.6
	Non-tortuosity			34	25.4
Anastomosis	Rectal Anastomosis	3	7	10	16.1
	Penile Anastomosis	7	8	15	24.2
	Bladder Anastomosis	3	4	7	11.3
	Contralateral Anastomosis	15	15	30	48.4
	Total			62 (100%)	

Table 3. Classification of PAs by Shape and Anastomosis

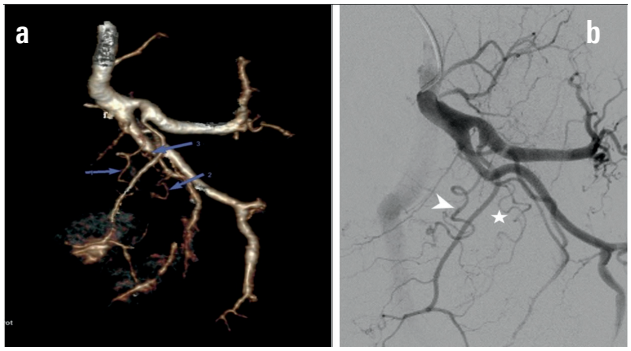

Figure 1. DECT and DSA images of the internal iliac artery in a patient with 2 left prostatic arteries. (a) 3D rendering of the left internal iliac artery in same-side anterior oblique projection (35°), the prostatic artery 1 (arrow 1) separated from the common trunk of the superior vesical artery, the prostatic artery 2 (arrow 2) separates from the internal pudendal artery, seminal vesicle artery (arrow 3). (b) angiogram of the left internal iliac artery in same-side anterior oblique projection (35°), prostatic artery 1 (arrowhead), prostatic artery 2 (star).

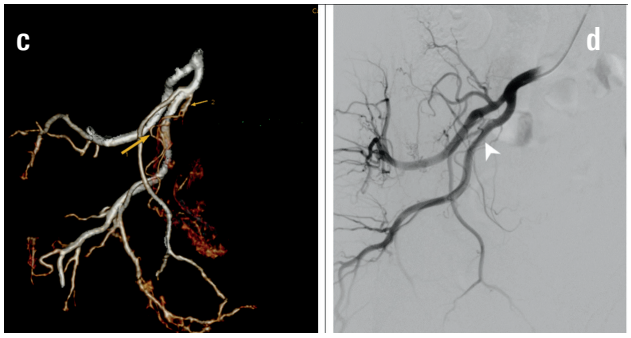

Figure 2. DECT and DSA images of the internal iliac artery in a patient with one right prostatic artery. (c) 3D rendering of the right internal iliac artery artery in same-side anterior oblique projection (40°), the prostatic artery (arrow 1) separates directly from the anterior trunk of the internal iliac artery, below the separation. of the superior vesical artery (arrow 2). (d) angiogram of the right internal iliac in same-side anterior oblique projection (40°), right prostatic artery (arrowhead).

The PAs tortuosity was observed in 74.6% of cases (n=99). The non-tortuous PAs were observed in 25.4% of cases (n=34). The contralateral anastomoses were dominant (48.4%), followed by the penile anastomoses and rectal anastomoses.

5. DISCUSSION

Dual-energy computed tomography (DECT) is a technological advancement in imaging diagnosis which provides valuable information in assessing very small blood vessels such as the PAs, Adamkiewicz artery, and dorsal penile artery (6, 7). Additionally, DECT was especially advantageous in the bone subtraction option, creating favourable conditions to obtain optimal multi-dimensional images for vascular assessment (8). DECT with the 3D reconstruction of the PAs has allowed the depicting of high-quality images of PA anatomy, tortuosity, diameter, degree of atherosclerosis, and anastomoses, particularly the ability to visualize the expected angle view of the PA root preoperatively. Thus, preoperative DECT imaging of the PAs can help narrow down interventional duration and reduce radiation exposure for both patients and interventionalists. In our search of medical literature, there was no paper focusing on DECT imaging in the assessment of PA anatomy before BPH embolization. Therefore, we performed a study to evaluate the value of DECT with 3D reconstruction of PAs in attempting to describe PA anatomy before PAE.

The average age of patients in our study was 67.3 ± 7.8 years which is similar to studies by T. Bilhim (9) and Wang (10). This age group is considered a high-risk group due to multiple accompanying conditions like hypertension, diabetes, and heart failure. This fact is a strong suggestion for minimally invasive intervention methods as a reasonable choice to avoid potential surgical complications.

Additionally, according to the study by Han et al. (11), age affects the degree of tortuosity and the rate of atherosclerosis in PAs, leading to increased intervention duration and radiation dose. The average prostate volume in our study was 72.3±12.6 ml, which is lesser than the results of studies by N. Kisilevzky (12) and T. Bilhim (9). This can be explained by the diversion of stature in the sample populations of Vietnamese people compared to the worldwide population. The study by Wang et al. (10) in 2015 successfully performed embolization for patients with prostate volume > 80 grams which directly proved the safe and effective characterization of PAE in this ethnic group (13). Therefore, embolization is a promising method for patients with large prostate volumes who are contraindicated or unresponsive for surgery. In our study, the average IPSS score was 22.2±5.5, indicating severe obstruction and the average QoL score was 3.4±2.6, corresponding to an acceptable quality of life. These numbers are consistent with the criteria for indicating PAE for BPH treatment. The average total PSA concentration in our study was slightly elevated (12.4±5.6), possibly due to factors such as urinary tract infection, prostatitis, post-biopsy or post-prostate surgery, medication use, or transrectal ultrasound of the prostate (14).

The incidence rate of 02 PAs on a pelvic side in our study was 3.9%, lower than the research of FC. Carnevale (5) (8%) and T. Bilhim (9) (43%). Several extremely rare anatomic variants did not appear in our paper encompassing 02 PAs on both pelvic sides or 03 PAs on the same pelvic side. In contrast, T. Bilhim (9) reported some patients with 02 PAs on both pelvic sides and 4% of cases with 03 PAs on the same pelvic side. In the case of 02 PAs on the same pelvic side, the anterior–superior branch usually originates from the common trunk with a superior vesical artery and supplies for the central part of the prostate; the posterior-inferior branch usually arises from the internal pudendal artery or obturator artery which supplies to the periphery of the gland. In fact, embolizing one of these two upper branches is acceptable due to their likelihood of connection with each other inside the gland. The anterior-superior branch supplies blood to the centre of the gland, and the hyperplastic nodules should be the priority for occlusion (10). However, the anterior–superior branch is often difficult to access as the high frequency of branches from the superior vesical artery at a narrow angle and tortuosity, especially in combination with atherosclerosis (10). FC. Carnevale was the pioneer to propose the classification of PAs by origin, encompassing 5 groups of separating roots: common trunk with the superior vesical artery (type I), anterior division of the internal iliac artery, inferior to the superior vesical artery (type II), obturator artery (type III), internal pudendal artery (type IV), and other locations (type V) (5).

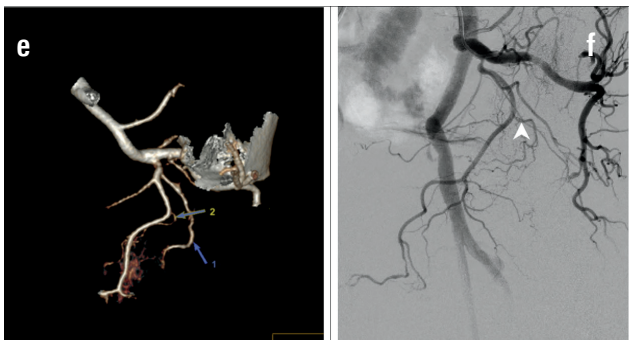

Figure 3. DECT and DSA images of the internal iliac artery in a patient with one left prostatic artery. (e) 3D rendering of the left internal iliac artery in same-side anterior oblique projection (40°), the prostatic artery (arrow 2) separates from the obturator artery, below the separation of the internal pudendal artery (arrow 1). (f) angiogram of the left internal iliac artery in same-side anterior oblique projection (40°), left prostatic artery (arrowhead).

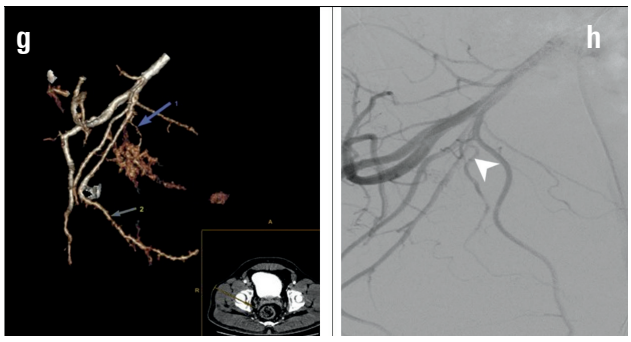

Figure 4. DECT and DSA images of the internal iliac artery in a patient with one right prostatic artery. (g) 3D rendering of the right internal iliac artery in in same-side anterior oblique projection (50°), the prostatic artery (arrow 1) separates from the internal pudendal artery (arrow 2). (h) angiogram of the left internal iliac artery in same-side anterior oblique projection (50°), left prostatic artery (arrowhead)

Our results suggest that PAs originating the typical origin arising from the common trunk with the superior vesical artery (29.6%) (Figure 1), followed by obturator artery (24.6%) (Figure 3) and the internal pudendal artery (23.7%) (Figure 4). According to the investigation of Enderlein et al. (15), the most common origins are the common trunk with superior vesical artery (27.5%), followed by obturator artery (23.8%) and the internal pudendal artery (23.1%), which is similar to our results. However, FC. Carneval (5) and T. Bilhim (9) reported that the most common origins were from the obturator artery (corresponding rates of 31.1% and 34.1%, respectively), followed by the common trunk with the superior vesical artery (corresponding rates of 28.7% and 20.1%, respectively). We habor the idea that our study of the different popular samples is responsible for the separation of PA anatomical variations. On DECT images, determining the origin of the PA is based on the image of the artery pathway from the parenchyma to the origin. Reconstruction of 3D images and multi-planes locating points of DECT facilitate the ability to determine the origin of the PA in cases arising from the anterior branch of the internal iliac artery located close to the body of the superior vesical artery compared to DSA (Figure 2). Less common origins of PAs include the middle rectal artery, superior gluteal artery, inferior gluteal artery, accessory pudendal artery, and accessory obturator artery. Our study had 8 cases of PAs originating from rare locations, including 2 cases from the accessory pudendal artery, 5 cases from the accessory obturator artery, and 1 case originating from the superior rectal artery branch of the inferior mesenteric artery, which is very rare. This anatomical variation is unique in our study and previous reports of PAE. The incidence rate of all rare root locations in our study was 6.7% which is in accordance with FC. Carnevale's study (5), and significantly lower than T. Bilhim's study (9).

Another challenge in PAE delivery is the presence of atherosclerosis, which makes the selection process of PAs more difficult, directly affecting the outcome of the embolisation technique. Our study found that the rate of atherosclerosis in the origins of the PAs was 24.6%, with an average diameter of the PAs of 1.5 mm (consistent with the results of studies by Bilhim (9) and Wang (10). Due to the small size of the PA and the gradual decrease in diameter, the average diameter of each PA in our study was calculated as the average diameter of three positions: the origin, the branching point, and the mid-point between these two positions. According to Bilhim (9), the PAs had small diameters ranging from 1-2 mm, depending on the number of PAs per pelvic side. Patients with single PAs on each pelvic side tend to have larger diameters (about 2 mm), while those with double PAs on each pelvic side tend to have smaller diameters (about 1 mm) (9). Furthermore, Wang (10) reported that patients with larger total prostate volumes (≥80 ml) had larger PA diameters compared to those with smaller average prostate volumes (<80 ml). By determining the diameter of the PAs before embolisation, we can determine the proper size of the microcatheter and embolic particles.

In our study, PAs were considered tortuous when they had one or more twists, accounting for 74.6% of cases, higher than Bilhim's study (9). The high prevalence of tortuous PAs may be due to the common occurrence of tortuosity in elderly patients and may be related to increased proliferation of glandular tissue (10). Tortuous vessel images can be considered a point of reference for identifying PAs on DSA. Posterior to the origin, the PA will curve downward and inward, then forward towards the base of the bladder. Sometimes, the PAs can give branches to the bladder neck before feeding the prostate parenchyma. Therefore, it is necessary to limit the amount of embolic particles at the proximal part of the PA, as it may obstruct bladder-feeding branches, leading to hemorrhagic necrosis of the bladder. However, if the selection of the PA is too deep before infusion, some supply branches of the prostate parenchyma may be neglected.

The most common anastomosis in this paper was contralateral PA, caused by branches supplying the central region of the prostate. This also explains cases where only one side was embolised, but the effectiveness could have been more significantly diverse with embolising both sides. Among these anastomoses, half of the cases were small anatomical branches, often appearing after partially embolising the ipsilateral PA or too small to be selected. In such cases, using larger-sized particles and slow, controlled infusion under fluoroscopic guidance is necessary to avoid unintentional obstruction of these branches. In the remaining half of cases, there were larger anastomoses, requiring selective occlusion of the base

of these anastomoses with coils. Branches supplying the central region of the prostate have penile anastomoses and contralateral anastomoses, while branches supplying the peripheral area of the prostate sometimes have anastomoses with the seminal vesicles, rectum, muscles, and skin nearby. Due to the increased angiogenesis in enlarged prostates, each PA may simultaneously provide multiple anastomoses to nearby organs.

Limitation of the study

The limitations of our study include lacking ConeBeam CT during PA selection on DSA. ConeBeam CT may be applicable to confirm the exact position of the main conduit in the target PA before embolisation, especially in suspicious cases. However, we believe routine use is optional if DECT with PA reconstruction has been performed before the intervention and the interventional radiologist has extensive experience in PAE. Other limitations relate to the variability in the classification of the origin of the PA depending on the anatomical classification used. Additionally, there may be small anastomoses of the PAs that DECT does not detect. Future studies with larger sample sizes to evaluate anastomoses using ConeBeam CT in the procedure could also contribute to this topic.

6. CONCLUSION

PAs have highly variable origins side by side, person to person and most frequently arise from the internal pudendal artery.

Dual-energy computed tomography (DECT) with 3D reconstruction of the PA facilitates accurately describing the anatomy of the PA, providing valuable information before intervention, such as the number, anatomical variants, atherosclerosis, diameter, tortuosity, and anastomoses.

- **Ethical approval:** Hanoi Medical University's institutional review board supported this study. This study was conducted according to the ethical standards of the 1964 Declaration of Helsinki and its later amendments.
- **Informed consent:** The requirement for informed consent was obtained.
- **Availability of data and materials:** The datasets generated and/or analysed during the current study are not publicly available due to privacy concerns but are available from the corresponding author on reasonable request.
- **Author's contribution:** The all authors were involved in all steps of preparation this article, including final proofreading.
- **Conflict of interest:** The authors declare no conflict of interests.
- **Financial support and sponsorship:** This research received no external funding.

REFERENCES

1. Young S, Golzarian J. Prostatic artery embolization for benign prostatic hyperplasia: a review. Curr Opin Urol. 2018; 28(3): 284-2287. doi:10.1097/MOU.0000000000000495
2. Pisco JM, Pinheiro LC, Bilhim T, Duarte M, Mendes JR, Oliveira AG. Prostatic arterial embolization to treat benign prostatic hyperplasia. J Vasc Interv Radiol. 2011; 22(1): 11-19; quiz 20. doi:10.1016/j.jvir.2010.09.030
3. Pisco JM, Bilhim T, Pinheiro LC, et al. Medium- and Long-Term Outcome of Prostate Artery Embolization for Patients with Benign Prostatic Hyperplasia: Results in 630 Patients. J Vasc Interv Radiol. 2016; 27(8): 1115-1122. doi:10.1016/j.jvir.2016.04.001
4. Bilhim T, Casal D, Furtado A, Pais D, O'Neill JEG, Pisco JM. Branching patterns of the male internal iliac artery: imaging findings. Surg Radiol Anat. 2011; 33(2): 151-159. doi:10.1007/s00276-010-0716-3
5. Carnevale FC, Soares GR, de Assis AM, Moreira AM, Harward SH, Cerri GG. Anatomical Variants in Prostate Artery Embolization: A Pictorial Essay. Cardiovasc Intervent Radiol. 2017; 40(9): 1321-1337. doi:10.1007/s00270-017-1687-0
6. Ghasemi Shayan R, Oladghaffari M, Sajjadian F, Fazel Ghaziyani M. Image Quality and Dose Comparison of Single-Energy CT (SECT) and Dual-Energy CT (DECT). Radiol Res Pract. 2020; 2020: 1403957. doi:10.1155/2020/1403957
7. Vlahos I, Chung R, Nair A, Morgan R. Dual-energy CT: vascular applications. AJR Am J Roentgenol. 2012; 199(5 Suppl): S87-97. doi:10.2214/AJR.12.9114
8. Bie Y, Yang S, Li X, Zhao K, Zhang C, Zhong H. Impact of deep learning-based image reconstruction on image quality compared with adaptive statistical iterative reconstruction-Veo in renal and adrenal computed tomography. J Xray Sci Technol. 30(3): 409-418. doi:10.3233/XST-211105
9. Bilhim T, Pisco JM, Rio Tinto H, et al. Prostatic arterial supply: anatomic and imaging findings relevant for selective arterial embolization. J Vasc Interv Radiol. 2012; 23(11): 1403-1415. doi:10.1016/j.jvir.2012.07.028
10. Wang MQ, Duan F, Yuan K, Zhang GD, Yan J, Wang Y. Benign Prostatic Hyperplasia: Cone-Beam CT in Conjunction with DSA for Identifying Prostatic Arterial Anatomy. Radiology. 2017; 282(1): 271-280. doi:10.1148/radiol.2016152415
11. Han EA, Nandalur KR, Morgan MA, et al. MRI of Benign Prostatic Hyperplasia: Important Pre- and Posttherapeutic Considerations. Radiographics. 2023; 43(5): e220096. doi:10.1148/rg.220096
12. Kisilevzky N, Faintuch S. Is prostatic artery embolization similar to uterine artery embolization? Cardiovasc Intervent Radiol. 2015; 38(1): 247-250. doi:10.1007/s00270-014-0874-5
13. Heidenreich A, Bastian PJ, Bellmunt J, et al. EAU guidelines on prostate cancer. part 1: screening, diagnosis, and local treatment with curative intent-update 2013. Eur Urol. 2014; 65(1): 124-137. doi:10.1016/j.eururo.2013.09.046
14. Distler FA, Radtke JP, Bonekamp D, et al. The Value of PSA Density in Combination with PI-RADSTM for the Accuracy of Prostate Cancer Prediction. J Urol. 2017; 198(3): 575-582. doi:10.1016/j.juro.2017.03.130
15. Enderlein GF, Lehmann T, von Rundstedt FC, et al. Prostatic Artery Embolization-Anatomic Predictors of Technical Outcomes. J Vasc Interv Radiol. 2020; 31(3): 378-387. doi:10.1016/j.jvir.2019.09.005
16. du Pisanie J, Abumoussa A, Donovan K, Stewart J, Bagla S, Isaacson A. Predictors of Prostatic Artery Embolization Technical Outcomes: Patient and Procedural Factors. J Vasc Interv Radiol. 2019; 30(2): 233-240. doi:10.1016/j.jvir.2018.09.014